FEMS Microbiology Ecology, 2023, 99, 1–14
DOI: 10.1093/femsec/fiac156
Advance access publication date: 9 January 2023
Research Article

Mixotrophy broadens the ecological niche range of the iron oxidizer *Sideroxydans* sp. CL21 isolated from an iron-rich peatland

Rebecca E. Cooper[1], Jessica Finck[1], Clara Chan[2,3,4], Kirsten Küsel[1,5,*]

[1]Aquatic Geomicrobiology, Institute of Biodiversity, Friedrich Schiller University Jena, 07743 Jena, Germany
[2]School of Marine Science and Policy, University of Delaware, Newark, DE 19716, United States
[3]Delaware Biotechnology Institute, University of Delaware, Newark, DE 19713, United States
[4]Department of Earth Sciences, University of Delaware, Newark, DE 19716, United States
[5]German Centre for Integrative Biodiversity Research (iDiv) Halle-Jena-Leipzig, 04103 Leipzig, Germany
*Corresponding author. Institute of Biodiversity, Friedrich Schiller University Jena, Dornburger Str. 159, 07743 Jena, Germany. Tel: +49 3641 949461; Fax: +49 3641 949462; E-mail: kirsten.kuesel@uni-jena.de
Editor: Tillmann Lueders

Abstract

Sideroxydans sp. CL21 is a microaerobic, acid-tolerant Fe(II)-oxidizer, isolated from the Schlöppnerbrunnen fen. Since the genome size of *Sideroxydans* sp. CL21 is 21% larger than that of the neutrophilic *Sideroxydans lithotrophicus* ES-1, we hypothesized that strain CL21 contains additional metabolic traits to thrive in the fen. The common genomic content of both strains contains homologs of the putative Fe(II) oxidation genes, *mtoAB* and *cyc2*. A large part of the accessory genome in strain CL21 contains genes linked to utilization of alternative electron donors, including NiFe uptake hydrogenases, and genes encoding lactate uptake and utilization proteins, motility and biofilm formation, transposable elements, and pH homeostasis mechanisms. Next, we incubated the strain in different combinations of electron donors and characterized the fen microbial communities. *Sideroxydans* spp. comprised 3.33% and 3.94% of the total relative abundance in the peatland soil and peatland water, respectively. Incubation results indicate *Sideroxydans* sp. CL21 uses H_2 and thiosulfate, while lactate only enhances growth when combined with Fe, H_2, or thiosulfate. Rates of H_2 utilization were highest in combination with other substrates. Thus, *Sideroxydans* sp. CL21 is a mixotroph, growing best by simultaneously using substrate combinations, which helps to thrive in dynamic and complex habitats.

Keywords: *Sideroxydans* sp. CL21, genome, physiology, peatland, iron oxidation, mixotrophy

Introduction

Gallionellaceae iron-oxidizing bacteria (FeOB) perpetuate the iron cycle at the oxic-anoxic interface in many freshwater ecosystems (Weber *et al.* 2006). FeOB usually have a narrow range of known ecological functions and are typically cultivated as microaerophilic chemolithoautotrophs, using Fe(II) as the electron donor coupled to the reduction of O_2 and fixing CO_2. The Gallionellaceae *Gallionella* and *Sideroxydans* are two of the most abundant and well-studied FeOB genera (Emerson *et al.* 2010, Fleming *et al.* 2014 , Zhou *et al.* 2022), and these two genera are composed of fewer than 10 known species, of which all have the ability to oxidize Fe(II). Although a close evolutionary relationship between members of the family Gallionellaceae has been established, strains from diverse habitats exhibit differences in the genetic content (Bethencourt *et al.* 2020). Adaptive microorganisms often exhibit higher metabolic flexibility which enables these microorganisms to inhabit more diverse and previously inaccessible niches (Roller and Schmidt 2015, Carere *et al.* 2017, Eggerichs *et al.* 2020).

We isolated the FeOB *Sideroxydans* sp. CL21 from a moderately acidic, Fe-rich peatland, the Schlöppnerbrunnen fen (Lüdecke *et al.* 2010). This strain seems to be well adjusted to its environment, as it prefers pH 5.5 rather than pH neutral conditions like the neutrophilic model FeOB *Sideroxydans lithotrophicus* ES-1, isolated from iron-rich groundwater (Emerson and Moyer 1997). *Sideroxydans* sp. CL21 can also tolerate higher oxygen concentrations than *S. lithotrophicus* ES-1, which enables this strain to thrive even in the upper oxic layer of the peatland soil (Kügler *et al.* 2019). FeOB in peatlands are exposed to fluctuating environmental conditions compared to those thriving in aquatic systems, like ground water or streams (Chan *et al.* 2016, Yang *et al.* 2021). In semi-terrestrial habitats, a huge variety of electron donors and acceptors can coexist in a three-dimensional structured matrix.

Peatlands are poorly drained areas with the capacity to accumulate significant amounts of CO_2-derived carbon in a recalcitrant form that approximates 30% of land-based organic carbon (Bragazza *et al.* 2013, Mitra *et al.* 2014). Mineralization in peatlands leads to methanogenesis with CO_2 as a terminal electron acceptor, when oxygen, nitrate, oxidized iron and sulfate become depleted (Knorr and Blodau 2009, Wu¨st et al. 2009). The groundwater fed Schlöppnerbrunnen fen is subjected to frequent water table fluctuations, and its biogeochemistry, redox processes and microbial communities have been well studied over the past several decades (Blodau *et al.* 2002, Alewell *et al.* 2006, Bodelier *et al.* 2006, Paul *et al.*

Received: August 3, 2022. **Revised:** November 17, 2022. **Accepted:** January 6, 2023

2006, Küsel *et al.* 2008, Reiche *et al.* 2008, Pester *et al.* 2010). Typical fermentation products, including formate, acetate, lactate, succinate, and H_2, have been detected in peatland water samples taken from the Schlöppnerbrunnen fen and during anoxic peatland soil incubation studies (Hamberger *et al.* 2008, Küsel *et al.* 2008, Wu¨st *et al.* 2009, Hädrich *et al.* 2012). *S. lithotrophicus* ES-1 is not known to utilize lactate, however, amendment with lactate and H_2 appeared to stimulate activities of *Sideroxydans* sp. CL21 (Cooper *et al.* 2020b). Various reduced S species have also been measured in this fen, including dissolved sulfides ($\sum H_2S$) (0.2–29 μM) and thiosulfate (30–90 μM) (Hädrich *et al.* 2019). Since *S. lithotrophicus* ES-1 does contain the genetic potential for thiosulfate oxidation via the *sox pathway*, electron donors other than Fe(II) might also be used by *Sideroxydans* sp. CL21.

Due to the relatively low number of publicly available genome sequences of isolated members of the family Gallionellaceae, few studies have extensively studied and characterized the metabolic and genetic diversity of these FeOB (Emerson *et al.* 2013, He *et al.* 2017, Bethencourt *et al.* 2020, Garber *et al.* 2020, McAllister *et al.* 2020, Huang *et al.* 2022). We recently reported the draft genome sequence of *Sideroxydans* sp. CL21, highlighting genes involved in Fe(II), sulfur, and H_2 oxidation (Cooper *et al.* 2020a). *Sideroxydans lithotrophicus* ES-1 and *Sideroxydans* sp. CL21 share a high degree of homology between the genes encoding the Fe(II) oxidation machinery. However, a brief comparison of the *Sideroxydans* sp. CL21 and *S. lithotrophicus* ES-1 genome sequences revealed the genome size of strain CL21 is 21% larger than *S. lithotrophicus* ES-1 (Cooper *et al.* 2020a). We hypothesized that CL21 is particularly adjusted to specific conditions of this peatland and contains additional metabolic traits to utilize an array of both inorganic and organic substrates. We compared the genomes of both FeOB to identify specific genes of strain CL21 to evaluate if *Sideroxydans* sp. CL21 has the genomic potential to utilize alternative electron donors, including H_2 or S species, as well as organic C sources in lieu of CO_2 fixation. Next, we set up incubation studies to verify some of these potentials and offered a combination of various electron donors to understand the preference of *Sideroxydans* sp. CL21. The combined strategy ultimately allows us to bring together genomic information, experimental evidence, and environmental characterizations of the Schlöppnerbrunnen fen to provide a more comprehensive description of this FeOB in relation to the environment in which it thrives.

Methods

Cultivation conditions of *Sideroxydans* sp. CL21

Sideroxydans sp. CL21 was isolated from the Schlöppnerbrunnen fen located in the Lehstenbach catchment area in the northern Fichtelgebirge region (Northern Bavaria, Germany; 50°07′54″N, 11°52′51″E) (Lüdecke *et al.* 2010). *Sideroxydans* sp. CL21 cultures were routinely cultivated in semi-solid gradient tubes containing 0.15% agarose-stabilized MWMM (top layer) (Biozyme LE Agarose; Biozyme Scientific GmbH, Hessisch Oldendorf, DE) and zero-valent Fe (Fe^0) or an FeS plug as the Fe source, in order to maintain stock cultures as previously described (Emerson and Moyer 1997, Lüdecke *et al.* 2010, Cooper *et al.* 2020b). For incubation studies, *Sideroxydans* sp. CL21 cultures were grown in semi-solid gradient (Emerson and Floyd 2005, Lüdecke *et al.* 2010, Cooper *et al.* 2020b) using ATCC medium 2672 (modified Wolfe's minimal media (MWMM)) amended with 10 mM MES buffer (pH 6.3), Wolfe's vitamin solution (10 ml L^{-1}), and Wolfe's mineral solution (10 ml L^{-1}) unless otherwise noted. Semi-solid incubations in Balch tubes were performed to determine utilization of supplemented H_2. *Sideroxydans* sp. CL21 stock cultures were used as inoculum for both semi-solid gradient incubations and liquid incubations (20–40 μl inoculum 6 ml^{-1} or 1 ml inoculum 100 ml^{-1}, respectively). For all incubations, 6 replicates were prepared along with 1 abiotic control. At predetermined intervals, samples were taken in triplicates for DNA extraction. All samples were stored at −20 °C until further use.

Semi-solid gradient tube incubations with either FeS or Fe^0 as the Fe source, were amended with 1 mM lactate or 1 mM acetate as an organic C source to test for mixotrophic growth over a 30-day incubation period. Lactate (5 mM) was also used in lactate-only incubations. NaS_2O_3 was amended as the reduced S source to test for sulfur oxidation. At predetermined intervals, samples were taken in triplicates for DNA extraction. All samples were stored at −20 °C until further use.

Semi-solid Balch tube incubations were used to monitor H_2 utilization as an alternative electron donor. Semi-solid Balch tube incubations were prepared with either FeS only, H_2 only (5%), or in combination (FeS and H_2, H_2 + lactate, FeS + H_2 + lactate). Balch tubes were inoculated with 40 μl inoculum and closed with a butyl rubber stopper. The H_2 only and FeS plus H_2 incubations were then amended with 1.1 ml sterile H_2 (~5% H_2 based on balch tube volume, media volume, and pre-selected pressure of 200 mbar). All incubations were prepared with or without amendment of organic C (1 mM lactate, peat water extract (PWE; Kügler et al. 2020), as previous experiments showed that PWE has a stimulatory effect on growth. At pre-determined intervals, samples from the gas phase or liquid phase (1 ml) were taken in triplicates with sterile syringes from all replicate tubes and used for DNA extraction, and GC analysis (H_2, O_2). Liquid samples were stored at −20 °C until further use.

Quantitative PCR (qPCR)

For quantitative PCR (qPCR), genomic DNA was extracted from semi-solid and liquid culture incubations. First, the cells were centrifuged at 5000 *g*, 10 min, 4°C. Next, genomic DNA from the cell pellets was extracted using a modified phenol-chloroform-based protocol (Taubert *et al.* 2018). The cell pellets were stored at −20°C until extraction, and genomic DNA was stored at −20 °C until further use.

qPCR analysis using the Sid-120F/Sid-167R primer pair (Fabisch *et al.* 2013) was conducted using genomic DNA extracts of samples taken from *Sideroxydans* sp. CL21 semi-solid and liquid incubations. Genomic DNA (2–20 ng) was used as template and the qPCR analysis was performed on an Mx3000P qPCR system (Agilent, Waldbronn, DE) with Maxima SYBR Green Master Mix (Thermo Fischer Scientific, Schwerte, DE). Standard curves using serial dilutions of representative plasmid mixtures ranging from 1×10^8 to 1×10^2 copies (R^2 value = 0.996–1.000) were linear and the qPCR was performed with efficiencies between 86% and 98%.

Gas chromatograph measurement and quantification of H_2 and O_2 gases

Headspace O_2 and H_2 concentrations in semi-solid Balch tube incubations were quantified using a Hewlett Packard 5890A series II gas chromatograph (GC) equipped with a molecular sieve column (Alltech #80II/2; 300 × 45.7 mm), a thermal conductivity detector (TCD) (model) with Ar as carrier gas (flow rate: 30 ml min^{-1}, 20 psi). The column, injector, and detector temperature settings were 50°C, 150°C, and 175°C, respectively. GC data was generated

and analyzed with the 32 Karat Software (v7.0, Beckman Coulter, Brea, US).

O_2 and H_2 concentrations in the headspace were calculated based on a derivation of the ideal gas law which includes measured O_2/H_2:

$$n_{gas} = \left(Y_i * P_i * V_{gas}\right) / \left(R * T\right) \quad (1)$$

where n_{gas} is the headspace O_2/H_2 concentration [mol per tube], Y_i is the measured O_2/H_2 concentration according to the standard curve, P_i is partial pressure [Pa], V_{gas} is the headspace volume [m^3], R is the general gas constant (8.314 [kPaL $mol^{-1}K^{-1}$]) and T is temperature [K].

O_2 and H_2 concentrations in the liquid or semi-solid phase were calculated based on a derivation of Henry's law which includes measured O_2/H_2 and liquid volume:

$$n_{liq} = Y_i * H_i * P_i * V_{liq} \quad (2)$$

where n_{liq} is the O_2/H_2 concentration [mol per tube] in the liquid phase, Y_i s the measured O_2/H_2 concentration according to the standard curve, P_i is partial pressure [Pa], V_{liq} is the liquid volume [L] and H_i is the respective Henry's law volatility constant [mol $m^{3\ -1}Pa^{-1}$]. H_i for O_2 ($1.30{\cdot}10^{-8}$) and H_2 ($7.70{\cdot}10^{-9}$) were taken from Sander (2015).

Comparative genomics of *Sideroxydans* sp. CL21 and *S. lithotrophicus* ES-1

We previously sequenced the draft genome of *Sideroxydans* sp. CL21 using the PacBio RS II platform (Pacific Biosciences, Menlo Park, CA) according to standard manufacturer's protocol (Cooper *et al.* 2020a) (GenBank accession: LR699166). The complete genome sequence of *S. lithotrophicus* ES-1 was retrieved from GenBank (accession: CP001965.1). The genome size of *Sideroxydans* sp. CL21 was 3.77 Mb and that of *S. lithotrophicus* ES-1 was 3.0 Mb. Completeness of both strains reached 99.37% and 99.52%, coding sequences were 3795 and 2996, and the GC content was 54.9 and 57.5%, respectively. Both strains had two copies of the 16S rRNA gene. Both genome sequences were annotated with RASTtk (v2.0) using default parameters (Aziz *et al.* 2008, Overbeek *et al.* 2014, Brettin *et al.* 2015). RAST predicted open reading frames (ORFs), which were later used for comparison of both genomes using the Anvi'o pangenomics workflow (described below). Initial pairwise genome comparisons were conducted using RAST. KEGG Decoder was used to perform initial assessments of pathways and metabolisms of interest as defined in the KO (KEGG Orthology) database. These assessments were performed using the script KEGG-decoder.py (www.github.com/bjtully/BioData/tree/master/KEGGDecoder) (Graham *et al.* 2018). ANI (average nucleotide identity) and AAI (average amino acid identity) were calculated using the *enveomics collection* (v0.1.3) (Rodriguez-R and Konstantinidis 2016). Orthologous protein cluster were identified using the *OrthoVenn* webserver (v 2, https://orthovenn2.bioinfotoolkits.net/) (Xu *et al.* 2019). Anvi'o v6.2 (Eren *et al.* 2015, Eren *et al.* 2021) was used to analyze the *Sideroxydans* sp. CL21 and *S. lithotrophicus* ES-1 genomes using the pangenomic workflow as previously described (Delmont and Eren 2018). The commands *anvi-run-ncbi-cogs* and *anvi-run-pfams* were implemented to annotate the contig database using NCBI's COG database and the Pfam database. The Pangenome analysis was performed using the command *anvi-pan-genome* and visualized using *anvi-display-pan*. The *anvi-pan-genome* command was run using the following parameters/flags:—num-threads 1;—minbit 0.5;—mcl-inflation 2; –use –diamond and—use-ncbi-blastp. The output of the Anvi'o Pangenome workflow was subsequently used for pairwise genome comparison of *Sideroxydans* sp. CL21 and *S. lithotrophicus* ES-1.

Microbial community composition analysis

Genomic DNA was extracted from either 5 cm increments of triplicate 30 cm soil cores or peatland water samples. Peatland water samples were collected in a depth-dependent manner in 5 cm increments in triplicates after peatland soil centrifugation or directly from a permanently installed pipe in the field, which serves as well for collection of higher volumes of water. Genomic DNA was extracted from both soil and water samples using the DNeasy PowerSoil Extraction kit (Qiagen) according to the manufacturer's protocol. Amplicon sequencing of bacteria and archaea 16S rRNA genes was carried out targeting the V4-V5 region using the Earth Microbiome Project primer pair, 515F-926R (Caporaso *et al.* 2011, Caporaso *et al.* 2012, Apprill *et al.* 2015, Parada *et al.* 2016). Illumina libraries were generated using the NEBNext Ultra II FS DNA library preparation kit (New England Biolabs) according to the manufacturer's protocol. Size selection was performed using the AMPure XP beads (Beckman Coulter). The sequencing was performed in-house using an Illumina MiSeq platform (v3 chemistry, 2 × 300 bp read lengths).

Amplicon sequence reads were initially subjected to primer sequence removal by cutting the 5' to 3' end based on primer sequence length. Read pairs were paired-end assembled and trimmed using *usearch* (v 10) (Edgar 2010) (settings paired-end assembly: -fastq_mergepairs; settings trimming: -fastx_truncate, -fastq_filter -fastq_maxee 1.0). Sequences were imported into *QIIME2* and subjected to dereplication, prior to clustering into operational taxonomic units (OTUs) using the implemented *vsearch* plugin (Rognes *et al.* 2016) and a sequence identity threshold of 97% (qiime vsearch cluster-features-de-novo). Low abundant OTUs (<10 sequence reads) were removed. Representative sequences were taxonomically assigned using the SILVA database (release 132) (Klindworth *et al.* 2013) and the *feature-classifier* plugin of *QIIME2* (qiime feature-classifier classify-consesus-vsearch). An OTU table including determined taxonomic affiliations and available metadata was assembled with QIIME2 (v 2019.10). Relative abundances at the genus level were exported using the *qiime taxa collapse* plugin. Data visualization of the relative abundances of the Fe(II) oxidizing bacteria in both soil and water fractions were carried out in the R framework for statistical analysis (v 1.3.959) (RStudio Team 2020), using the package *ggplot2* (Wickham 2016). Raw reads were deposited at the European Nucleotide Archive (ENA) under the BioProject accession PRJEB51207.

Results

Genome comparison of *Sideroxydans* sp. CL21 and the model neutrophilic FeOB *S. lithotrophicus* ES-1

To assess the genome similarities between *Sideroxydans* sp. CL21 and *S. lithotrophicus* ES-1, we examined the overlapping genomes of the two strains. The genomes of both strains species shared 2057 genes. *Sideroxydans* sp. CL21 contained a higher number of unique genes (i.e. the accessory genome) in comparison to *S. lithotrophicus* ES-1 (1270 and 784, respectively) (Table S1), which is consistent with the differences in genome sizes (3.77 Mb and 3.0 Mb, respectively). The average nucleotide identity (ANI) (82%) and average amino acid identity (AAI) (81.2%) (Rodriguez-R and Konstantinidis 2016) provided further evidence that *Sideroxydans* sp. CL21 and *S. lithotrophicus* ES-1 are distinct, but closely related species.

Pairwise comparisons of both strains using OrthoVenn2 identified a total of 2358 orthologous clusters, including 2242 overlapping orthologs.

To further understand important metabolic pathways for these strains individually, gene clusters (both shared and unique gene clusters) identified using the Anvi'o pangenome workflow were screened. Notably, shared gene clusters comprised of genes and pathways linked to Fe(II) oxidation, CO_2 fixation, dissimilatory sulfur oxidation, S, P, and N assimilation, Rnf complex, Alternative complex (AC) III, and electron transport were identified (Table S1). Gene clusters encoding for lactate utilization, motility, polysaccharide biosynthesis, biopolymer transport, pH homeostasis, and Ni-Fe-hydrogenase I were unique to the *Sideroxydans* sp. CL21 genome.

Fe(II) oxidation and electron transfer pathways in *Sideroxydans* sp. CL21

Genome analyses revealed homologous Fe(II) oxidation mechanisms in *Sideroxydans* sp. CL21 and *S. lithotrophicus* ES-1 (Liu *et al.* 2012, Emerson *et al.* 2013, Beckwith *et al.* 2015, He *et al.* 2017, Zhou *et al.* 2022). Both genomes include genes in the Cyc2 and Mto Fe(II) oxidation pathways, including homologs of *cyc2*, *mtoAB*, *cymA*, and *mtoD* (Keffer *et al.* 2021). The *Sideroxydans* sp. CL21 genome contains three copies of cyc2, as does *S. lithotrophicus* ES-1. Additional copies of genes encoding *cbb*$_3$-type cytochrome c oxidases were also found in the *Sideroxydans* sp. CL21 accessory genome. Genes encoding cytochrome *bd* ubiquinol oxidase subunits I and II (*cydAB*) were detected in both *Sideroxydans* strains (Fig 1A, Tables S1 and S2). Genes encoding a reverse electron transfer (RET) pathway, including NADH dehydrogenase, cytochrome *bc1*, and quinones were identified in the common genome content, as these genes are ubiquitous among iron oxidizers, which require RET for carbon fixation. Both genomes encode the alternative complex III (ACIII), which is suggested to participate in RET to provide reducing equivalents for the CO_2 fixation (Zhou *et al.* 2022), and also contain genes encoding a variety of cytochromes involved in electron transfer.

The *Sideroxydans* sp. CL21 genome also encodes an F-type ATPase as well as an N-type ATPase (Dibrova *et al.* 2010), which is a Na^+-translocating ATPase (Na^+-binding residues confirmed in subunit E). Genes encoding proteins involved in various redox reactions connected to the quinol pool were found in the core genome, however, strain CL21 harbored multiple copies of several of these genes, specifically those encoding electron transfer proteins (*etfAB*) and electron transfer flavoprotein ubiquinone oxidoreductase, in both the shared and accessory genome (Fig. 1A, Table S1).

Alternative energy metabolism pathways in *Sideroxydans* sp. CL21

In the *Sideroxydans* sp. CL21 accessory genome, we identified gene clusters linked to alternative electron transfer pathways, including H_2 oxidation genes and few genes for S oxidation. Genes linked to the regulation, assembly, and synthesis of Ni-Fe uptake hydrogenases were found and scattered across both the common genomic content and the *Sideroxydans* sp. CL21 accessory genome (Fig. 1A, Table S1). For example, a gene cluster in the *Sideroxydans* sp. CL21 accessory genome containing various genes encoding NiFe-hydrogenase I small subunit, Ni-Fe-hydrogenase I large subunit, Ni-Fe-hydrogenase maturation factor, hydrogenase expression protein, Ni-Fe-hydrogenase assembly proteins, and related accessory proteins (gene_callers_id(anvi'o): 602–611) were found in close localization to genes encoding a phage integrase family protein (gene_callers_id(anvi'o): 416) and the methionyl-tRNA formyltransferase/Enoyl-CoA hydratase enzyme, which functions as a transposase (gene_callers_id(anvi'o): 619), and are localized upstream and downstream of the gene cluster. Similarly, genes coding for an integrase and transposase are located upstream and downstream (gene_callers_id(anvi'o): 1012, 1283) of another NiFe-hydrogenase gene cluster encoding a HupF/HypC-family hydrogenase maturation factor, Ni-Fe-hydrogenase maturation factor, Ni-Fe-hydrogenase I small and large subunits, Ni-Fe-hydrogenase 2 integral membrane subunits (gene_callers_id(anvi'o): 1082–1087). This finding suggests that the capacity to utilize H_2 as an alternative electron donor to Fe(II) by *Sideroxydans* sp. CL21 was acquired via horizontal gene transfer. Homologs of dissimilatory sulfur oxidation pathway and other genes linked to S oxidation were also detected (Fig. 1A, Table S1).

Carbon metabolism genes in *Sideroxydans* sp. CL21 suggests a mixotrophic lifestyle

Sideroxydans sp. CL21 contains the genetic potential for both inorganic carbon fixation and organic carbon utilization. Briefly, the common genomic content contains genes encoding for CO_2 fixation, notably a complete Calvin-Benson-Bassham cycle (CBB pathway) (Fig. 1B, Table S1). Interestingly, strain CL21 also encodes genes linked to organic carbon (i.e. lactate) utilization pathways (Fig. 1B, Table S1). Genes encoding a predicted pathway for lactate oxidation in *Sideroxydans* sp. CL21 were identified across the shared and accessory genomes. Genes encoding the *L*-lactate dehydrogenase subunits are all located in the common genomic content (Fig. 1B, Table S1), while other key genes involved in lactate utilization, for example genes encoding a lactate permease, *D*-lactate dehydrogenase, acetate kinase, and acetate permease, were all found in the *Sideroxydans* sp. CL21 accessory genome (Fig. 1B, Table S1). Both *Sideroxydans* sp. CL21 and *S. lithotrophicus* ES-1 genomes encode complete pathways linked to other central metabolic processes, including the tricarboxylic acid (TCA) cycle and glycolysis (Entner-Doudoroff [ED] pathway) (Fig. 1B, Table S1).

Additional nutrient assimilation pathways in *Sideroxydans* sp. CL21

Both *Sideroxydans* sp. CL21 and *S. lithotrophicus* ES-1 can assimilate phosphorus via the *pho* regulon (Table S1). *Sideroxydans* sp. CL21 does not encode the entire phosphonate uptake and utilization pathway, similar to what is observed in the *S. lithotrophicus* ES-1 genome (Muhling *et al.* 2016). *Sideroxydans* sp. CL21 accessory genome contains genes encoding the putative transcriptional regulator (PhnF), phosphate import protein/substrate binding protein (PhnD/PtxB), phosphate-import ATP binding protein (PhnC), phosphate-import permease protein (PhnE), putative phosphonates utilization ATP-binding protein (PhnK), alpha-D-ribose 1-methylphosphonate 5-triphosphate synthase subunit (PhnL), phosphonate ABC-transporter, ATP-binding protein (PtxA), and an alkylphosphonate utilization protein (PhnA) (Table S1).

Similar to the genome of *S. lithotrophicus* ES-1, *Sideroxydans* sp. CL21 encodes genes linked to assimilation of ammonia, nitrate, and nitrite. Both strains also encode nitrogenase genes for nitrogen fixation (Table S1). According to the genome annotation, *Sideroxydans* sp. CL21 is not able to utilize urea as an alternative nitrogen source in the same way that other acidophilic microbes can (Hausinger 2004, Kanamori *et al.* 2005,

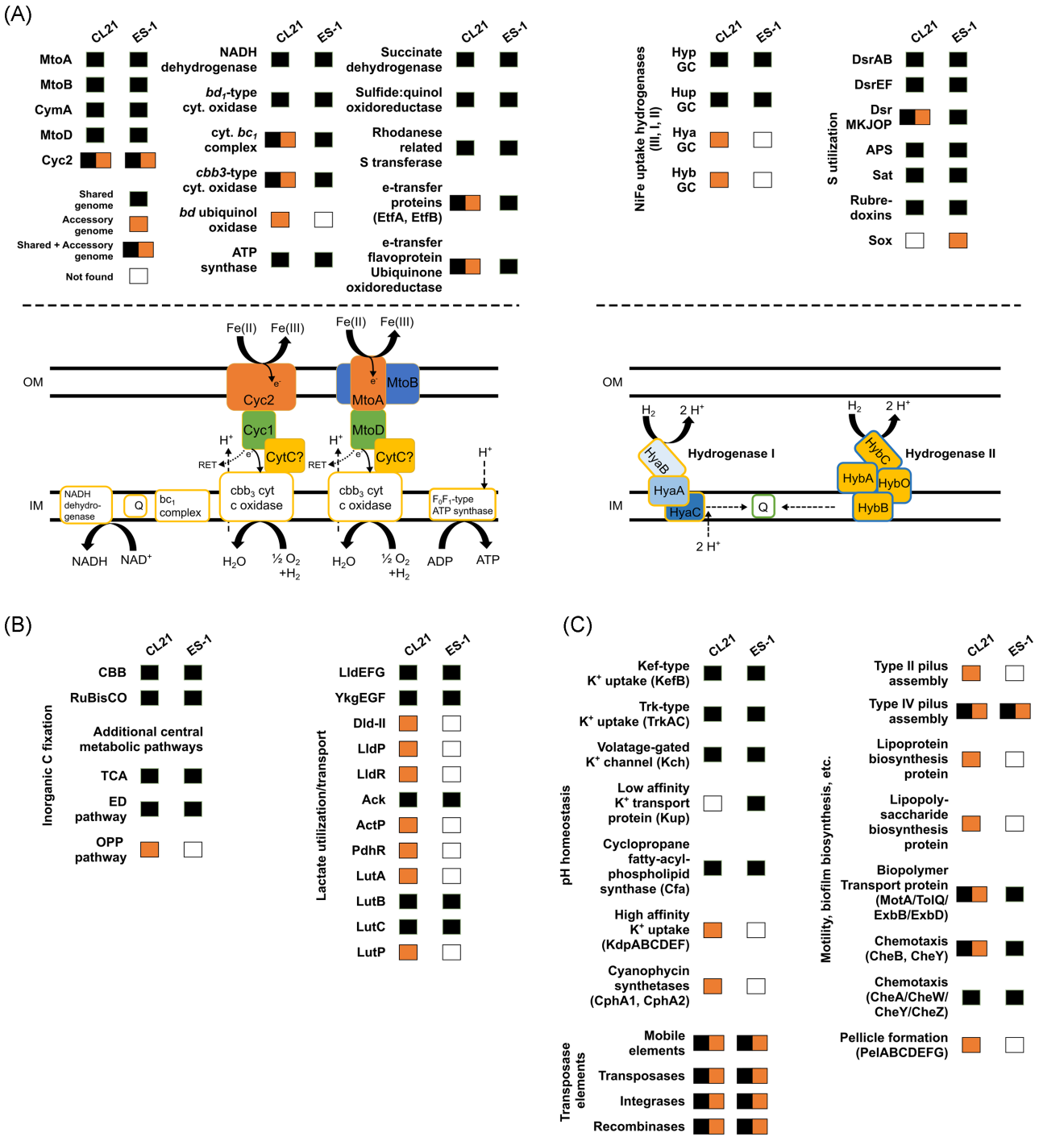

Figure 1. Schematic illustrating the similarities and differences in key metabolic pathways in *Sideroxydans* sp. CL21 and *S. lithotrophicus* ES-1. The schematic is based solely on genome comparison analyses. (**A**) Alternative electron donor pathways identified in *Sideroxydans* sp. CL21 and *S. lithotrophicus* ES-1. The proposed Fe(II) oxidation pathway is depicted in the left panel, and H_2 oxidation and S utilization and oxidation pathways are depicted in the right panel. Note, three copies of the *cyc2* gene are present in both strains and *S. lithotrophicus* ES-1 genome encodes genes linked to the complete Dsr pathways (*dsrABC, dsrEFHC, dsrMKLJOPN*), while *Sideroxydans* sp. CL21 does not. Two copies were located in the common genomic content, and a third copy of *cyc2* was identified in both the *Sideroxydans* sp. CL21 specific genome and the *S. lithotrophicus* ES-1 specific genome. (**B**) Inorganic C fixation pathways and lactate uptake/utilization pathways. (**C**) pH homeostasis and lifestyle-specific pathways (i.e. motility, biofilm). (black—gene in common genomic content; orange—gene in specific genome; black/orange—gene copy in common genomic content and specific genome; white—gene absent in common genomic content and specific genome).

Ullrich *et al.* 2016), as indicated by the lack of genes encoding the urea ABC transporter (*urtABC*). *Sideroxydans* sp. CL21 contains a partial urease gene cluster (urea carboxylase present), but genes encoding the allophanate hydrolase were not identified (Table S1).

pH homeostasis and other lifestyle adaptations in *Sideroxydans* sp. CL21

Sideroxydans sp. CL21 can tolerate more acidic pH conditions compared to the neutrophilic *S. lithotrophicus* ES-1. pH homeostasis in *Sideroxydans* sp. CL21 is likely maintained through a variety of

strategies, including Trk, Kch, Kup, and Kef-type potassium uptake systems and the Kdp high affinity potassium uptake system (Fig. 1C, Table S1). *Sideroxydans* sp. CL21 also encodes genes encoding two cyanophycin synthetases, which are known to function in pH homeostasis in cyanobacteria (Krehenbrink *et al.* 2002). Specific copies of genes and genetic pathways linked to motility and biofilm biosynthesis, and mobile elements, transposases, integrases, and recombinases were identified in the *Sideroxydans* sp. CL21 accessory genome (Fig. 1C, Table S1). For example, a transposase and an integrase located upstream and downstream of the high affinity potassium uptake system encoding the *kdpABCDEF* gene cluster, suggesting these genes were taken up from the environment.

Physiology of *Sideroxydans* sp. CL21: experimental characterization of alternative electron donor utilization

To experimentally verify the genomic potential of *Sideroxydans* sp. CL21, we incubated the isolate in the presence of alternative inorganic electron donors (H_2 and NaS_2O_3) and organic carbon and electron donors (lactate, acetate) and in various combinations (Fig. S1). Although *Sideroxydans* CL21 prefers to grow in semi-solid media supplemented with Fe^0 (Cooper *et al.* 2020b), we had to switch to FeS as the Fe source in some incubations, as H_2 is always released as a byproduct when Fe^0 reacts slowly with water forming Fe(II) and H_2 (Till *et al.* 1998).

All substrate combinations tested, except the combination of acetate and thiosulfate, stimulated growth of *Sideroxydans* CL21 in semi-solid media incubations amended with more than one inorganic electron donor or organic substrate. We also monitored growth in incubations amended with single substrates (FeS, H_2, NaS_2O_3, lactate, or acetate (data not shown)) as well as consumption of gases (Fig. 2, Table 1; Table S2). The 16S rRNA gene copies of *Sideroxydans* sp. CL21 increased by 3–4 orders of magnitude in FeS and H_2 only incubations. The 16S rRNA gene copies increased slightly in NaS_2O_3-only incubations, but did not show a significant change in lactate-only incubations (Fig. 2A, Table S2). H_2 was consumed with a rate of 0.637 μM d^{-1} during 18 days of incubation with a ratio of H_2 and O_2 consumption of nearly 1 : 1 (Fig. 2A, Table 1).

Next, we amended incubations with various combinations of two electron donors. Lactate and H_2 additions stimulated growth in the presence of FeS significantly. The 16S rRNA gene copy numbers increased between one and four orders of magnitude in incubations amended with FeS plus lactate or H_2 (Fig. 2B, Table S2). Similarly, 16S rRNA numbers increased approximately four orders of magnitude in incubations amended H_2 + lactate and NaS_2O_3 + lactate (Fig. 2B, Table S2). Lactate amendment in incubations with H_2 or NaS_2O_3 enhanced growth similarly to FeS + lactate incubations (Fig. 2B, Table S2). Compared to the H_2 only incubations, the rate of H_2 utilization increased 13% and 178% in incubations amended with FeS (FeS + H_2) and lactate (H_2 + lactate), respectively (Fig. 2B, Table 1).

Lastly, we monitored the effect of three electron donors in FeS + H_2 + lactate, Fe^0 + lactate, or Fe^0 + NaS_2O_3 incubations (Fig. 2C). The 16S rRNA gene copies increased almost five orders of magnitude in FeS + H_2 + lactate incubations and 3.5 orders of magnitude in Fe^0 + lactate (Fig. 2C, Table S2). The 16S rRNA gene copies decreased slightly in Fe^0 + NaS_2O_3 incubations (Fig. 2C, Table S2). The H_2 oxidation rate increased 1004% in incubations amended with FeS + H_2 + lactate (Fig. 2C, Table 1).

Abundance of *Sideroxydans* species in the Schlöppnerbrunnen fen

All known Fe(II)-oxidizers including *Sideroxydans* spp. made up to 3.33% of the percentage of the total read counts in the peatland soil and were found across all depths (0–30 cm). These relative abundances of *Sideroxydans* spp. increased with increasing depth from 0–5 cm to 25–30 cm (~0.01%–0.75%, respectively) (Fig. 3). Most Fe(II)-oxidizers had higher relative abundances in the peatland water and could reach 3.94%. In standing water sampled from an open permanently installed pipe in the field, total relative abundance of all Fe(II)-oxidizers reached 14.04% with more than 7% of *Sideroxydans* spp. This pipe water contained members of other genera of Fe-oxidizers, *Ferrovum and* other *Gallionella* species, and of the potential Fe-oxidizer *Crenothrix* (Otte *et al.* 2018, Cheng *et al.* 2019), which were not detected in peatland soil or peatland water (Fig. 3).

Discussion

Our combined genomic and experimental evidence demonstrates a broad metabolic flexibility of *Sideroxydans* sp. CL21, isolated from the Schlöppnerbrunnen fen. Its genome, which is ~21% larger than the genome size of its neutrophilic freshwater counterpart, *S. lithotrophicus* ES-1, isolated from groundwater from a basement tile drain in East Lansing, Michigan (Emerson and Moyer 1997) contains unique gene clusters encoding for organic carbon utilization, hydrogenase I system, motility, biofilm biosynthesis, and pH homeostasis, suggesting specific environmental conditions of the Schlöppnerbrunnen fen drive the difference in the genome content between both strains.

The Schlöppnerbrunnen fen is a groundwater-fed, minerotrophic peatland, completely overgrown with *Molinia* grasses and patches with *Carex* sedges (Meier *et al.* 2021), and receives lateral input of iron and sulfur species. Mean annual water table levels approximate 13 cm below soil surface (Knorr *et al.* 2009), but can drop down to > 70 cm in very dry summers (Paul *et al.* 2006). The peatland soil contains high amounts of solid iron (5–20 mg g wt $peat^{-1}$) and organic C (22%–55%) (Küsel *et al.* 2008, Reiche *et al.* 2010). The upper peat layer shows the highest abundance of solid phase Fe(III), that occurs mainly in the form of small-sized minerals resembling nanoparticulate ferrihydrite or goethite (Hädrich *et al.* 2019). In recent studies, the maximum concentrations of Fe(II) in peatland water samples reach 790 μM, and DOC concentrations range from 11 to 48 mg L^{-1} (Hädrich *et al.* 2019, Kügler *et al.* 2019). The majority of both Fe(III) and Fe(II) in this fen is complexed by DOM; complexed Fe(II) also occurs in the upper oxic peat layers (Kügler *et al.* 2019) due to stabilization similar to other studies (Riedel *et al.* 2013, Lee *et al.* 2017), as abiotic chemical oxidation of Fe(II) is inhibited. Similarly, acidic conditions inhibit chemical Fe(II) oxidation (Johnson *et al.* 2012, Ilbert and Bonnefoy 2013, Bryce *et al.* 2018). Thus, the Schlöppnerbrunnen fen with its high amounts of reduced, stabilized Fe in an organic rich, slightly acidic matrix exposed to fluctuating redox conditions is ideally suited to host microaerophilic FeOB.

Both *Sideroxydans* sp. CL21 and *S. lithotrophicus* ES-1 are microaerophilic FeOB. In the genomes of both *Sideroxydans* strains, we found genes for outer membrane cytochromes linked to Fe(II) oxidation, including *cyc2* and *mtoAB* (Liu *et al.* 2012, McAllister *et al.* 2020, Keffer *et al.* 2021). *Sideroxydans* sp. CL21 has three copies of the Fe(II) oxidation gene *cyc2* (Table S1) with one found in its accessory genome. The presence of at least two different Fe oxidases could allow flexibility to utilize multiple

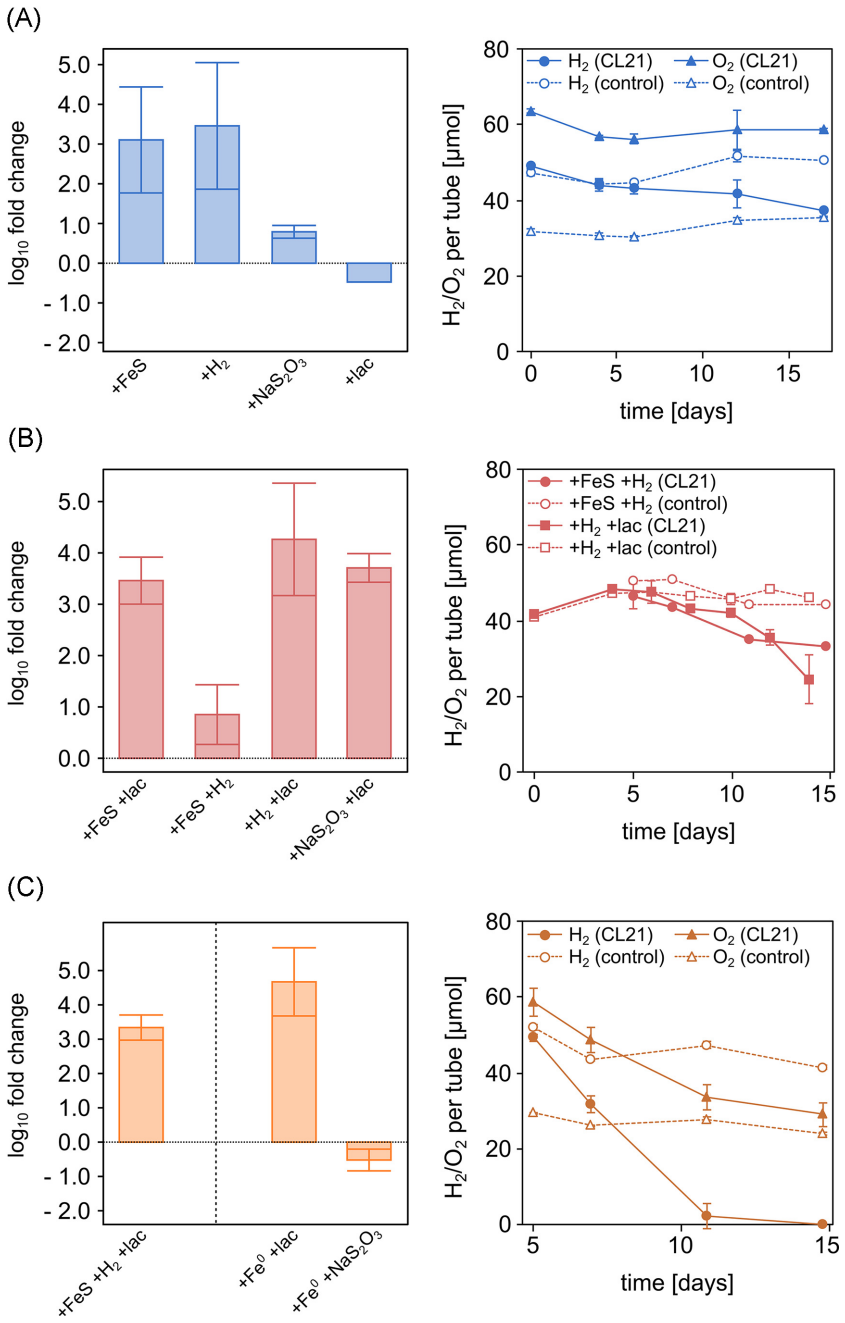

Figure 2. *Sideroxydans sp. CL21* semi-solid incubations amended with one, two, or three different electron donors or organic substrates. (**A**) Differences in 16S rRNA gene copies from T_{start} and T_{end}, shown as Log_{10} fold change (FC), in incubations amended with FeS, H_2, NaS_2O_3, or lactate as the sole electron donor (left panel). H_2 utilization and O_2 consumption in H_2-amended incubations [(CL21) refers to Sideroxydans sp. CL21 incubations; (control) refers to abiotic controls] (right panel). T_{start} = day 0; T_{end} = 17 d (NaS_2O_3, lactate) or 18 d (FeS, H_2). (**B**) Differences in 16S rRNA gene copies from T_{start} and T_{end}, shown as Log_{10} FC, in incubations amended with FeS + lactate, FeS + H_2, H_2 + lactate, or NaS_2O_3 + lactate (left panel). H_2 utilization in incubations amended with FeS + H_2 or H_2 + lactate is shown (right panel). T_{start} = day 0; T_{end} = 21 d (FeS + lactate), 19 d (FeS + H_2), 21 d (H_2 + lactate), 18 d (NaS_2O_3 + lactate). (**C**) Differences in 16S rRNA gene copies from T_{start} and T_{end}, shown as Log_{10} FC, in incubations amended with FeS + H_2 + lactate, Fe^0 + lactate, or Fe^0 + NaS_2O_3. H_2 utilization and O_2 consumption in incubations amended with FeS + H2 + lactate (right panel). T_{start} = day 0; T_{end} = 19 d (FeS + H_2 + lactate), 17 d (Fe^0 + lactate), and 18 d (Fe^0 + NaS_2O_3). Error bars represent standard deviation in triplicate incubations (n = 3). In some cases, error bars are smaller than the symbols.

Fe species. MtoA-based and Cyc2-based Fe(II) oxidation pathways transport electrons from Fe(II) across the outer membrane (OM) via cytochromes embedded in the OM to periplasmic proteins and finally to terminal oxidases in the inner membrane (IM) (Emerson *et al.* 2013, Beckwith *et al.* 2015, He *et al.* 2017). The presence of the Fe(II) oxidation machinery homologs, including *cymA*, in *Sideroxydans* sp. CL21 suggests a similar genetic organization to *S. lithotrophicus* ES-1. The *Sideroxydans* sp. CL21 genome encoded a *cbb3*-type cytochrome *c* oxidase, which has a high affinity for O_2 and suggests that it can grow in suboxic/microoxic environments (Pitcher *et al.* 2002, Li *et al.* 2014, Park *et al.* 2020). Thus, Fe(II) oxidation coupled to O_2 respiration can continue even as the O_2 concentrations in the peatland soil decline.

Table 1. H_2 and O_2 consumption rates in *Sideroxydans* sp. CL21 cultures grown in semi-solid gradient tube incubations with single, double, or triple electron donors.

Incubation set-up	H_2 consumption rate (μm d^{-1})	Average H_2 consumption rate (μm d^{-1})	O_2 consumption rate (μm d^{-1})	Average O_2 consumption rate (μm d^{-1})
H_2	0.632	0.637	0.764	0.484
	0.659		0.423	
	0.620		0.266	
FeS	NA		1.226	1.345
	NA	NA	1.934	
	NA		0.876	
H_2 + FeS	0.488	0.721	0.721	0.839
	0.978		1.025	
	0.696		0.772	
H_2 + lactate	1.865	1.774	1.346	1.306
	1.800		1.332	
	1.656		1.240	
H_2 + FeS + lactate	6.071	7.038	2.233	2.149
	7.631		2.506	
	7.411		2.519	

Sideroxydans sp. CL21 also encodes other genomic potentials to cope with O_2 level variations caused by the water table fluctuation in the fen. Previous work has shown that *Sideroxydans* sp. CL21 prefers to oxidize Fe(II) at O_2 concentrations up to 17.5% saturation, which is in the upper range observed for *S. lithotrophicus* ES-1 (5.5%–18.2%) (Druschel *et al.* 2008). Similar to *S. lithotrophicus* ES-1, *Sideroxydans* sp. CL21 has been shown to grow as a chemolithoautotroph (Lüdecke *et al.* 2010, Kügler *et al.* 2019, Cooper *et al.* 2020a). Both strains house two large subunit RuBisCO genes (Form I and II), suggesting that they can fix CO_2 also under high levels of O_2 in contrast to other microaerophilic FeOB (Emerson *et al.* 2013). Previous studies have shown that the Form I RuBisCo enzymes have a higher affinity for CO_2 compared to O_2, thus enabling CO_2 fixation at higher O_2 partial pressures compared to microbes encoding only Form II Rubisco enzymes (Badger and Bek 2008). Additionally, in strict microaerophiles, Form II enzymes likely do not encounter high enough O_2 levels to stimulate the oxygenase reaction compared to CO_2 fixation, which implies both strains are more tolerant to both O_2 fluctuations and overall higher O_2 concentrations (Emerson *et al.* 2013). We also identified genes encoding for O_2-tolerant Ni-Fe hydrogenases, involved in H_2 oxidation. Genes linked to the regulation, assembly, and synthesis of three types of Ni-Fe hydrogenases were present in both the common genomic content and the *Sideroxydans* sp. CL21 accessory genome. Since Ni-Fe hydrogenases are typically inhibited at atmospheric O_2 concentrations (Coppi *et al.* 2004, Shafaat *et al.* 2013, Peters *et al.* 2015), the presence of O_2-tolerant Ni-Fe hydrogenases in the accessory genome suggests adaptation to the microoxic conditions. These genes are homologous to O_2 tolerant membrane bound Ni-Fe-hydrogenases previously characterized in the β-proteobacterium *Ralstonia eutropha*, which is able to use H_2, CO_2, and O_2 for lithoautotrophic growth (Hartmann *et al.* 2018).

Dissolved H_2 concentrations in the Schlöppnerbrunnen fen range between 0.2–13 nM L^{-1} (Knorr and Blodau 2009); but these low concentrations are likely due to a rapid turnover of H_2, as it is a preferred substrate for the anaerobic electron-accepting processes dominating the Schlöppnerbrunnen fen, such as iron reduction, sulfate reduction, and methanogenesis (Knorr and Blodau 2009, Knorr *et al.* 2009). Moderately acid tolerant fermenters are involved in the carbon decomposition processes, leading to methane emissions of up to 13 mmol m^{-2} day^{-1} in this fen (Hamberger *et al.* 2008). The intermediary ecosystem metabolism (Drake *et al.* 2009) leads to the formation of the typical fermentation products H_2, formate, propionate, acetate, lactate, and succinate, all detected both in Schlöppnerbrunnen fen peatland water samples and during anoxic peatland soil incubation studies (Hamberger *et al.* 2008, Küsel *et al.* 2008, Wu¨st *et al.* 2009, Hädrich *et al.* 2012).

Our genomic data suggest that *Sideroxydans* sp. CL21 is a mixotroph, as it possesses all the genes for the utilization of organic carbon sources, like the fermentation product lactate (Fig. 4). Genes for a lactate oxidation pathway were identified across the shared and accessory genomes of strain CL21. As *S. lithotrophicus* ES-1 has not been predicted nor shown to oxidize lactate (Emerson and Moyer 1997, Emerson *et al.* 2010, Emerson *et al.* 2013), it appears to be an exclusive metabolic potential of *Sideroxydans* sp. CL21. *Sideroxydans* sp. CL21 provides another example of an FeOB within *Betaproteobacteria* that is not a strict autotroph. The presence of the oxidative TCA cycle as well as genes encoding for glucose degradation pathways, pyruvate metabolism, lactate dehydrogenases, lactate permease, acetate kinase, and acetate permease genes, suggests that *Sideroxydans* sp. CL21 can operate using a mixed energy metabolism and mixed carbon metabolism lifestyle. Many of these genes are only found in its accessory genome, suggesting that the extensive metabolic potential for organic nutrient utilization is a specific adaptation to an organic-rich habitat.

Our semi-solid incubation studies demonstrated that thiosulfate did appear to stimulate growth to the extent to which growth was stimulated in incubations amended with H_2 as an alternative electron donor. Genes for S oxidation, housed in the periplasm and inner membrane, were detected in both strains (Fig. 4). The *sox* pathway was found in *S. lithotrophicus* ES-1 and likely functions as the primary mechanism involved in sulfur oxidation in this strain (Emerson *et al.* 2013), however, the exact genes and pathway(s) involved in sulfur oxidation in *Sideroxydans* sp. CL21 could not be elucidated from the current genome annotation, however elucidating the genes and mechanisms involved in S metabolism in *Sideroxydans* species is essential for understanding the full metabolic potential of these microorganisms. In addition to thiosulfate, other reduced sulfur compounds present in the fen (Hädrich *et al.* 2019), could also function as potential electron donors for *Sideroxydans* sp. CL21. A high diversity of sulfate

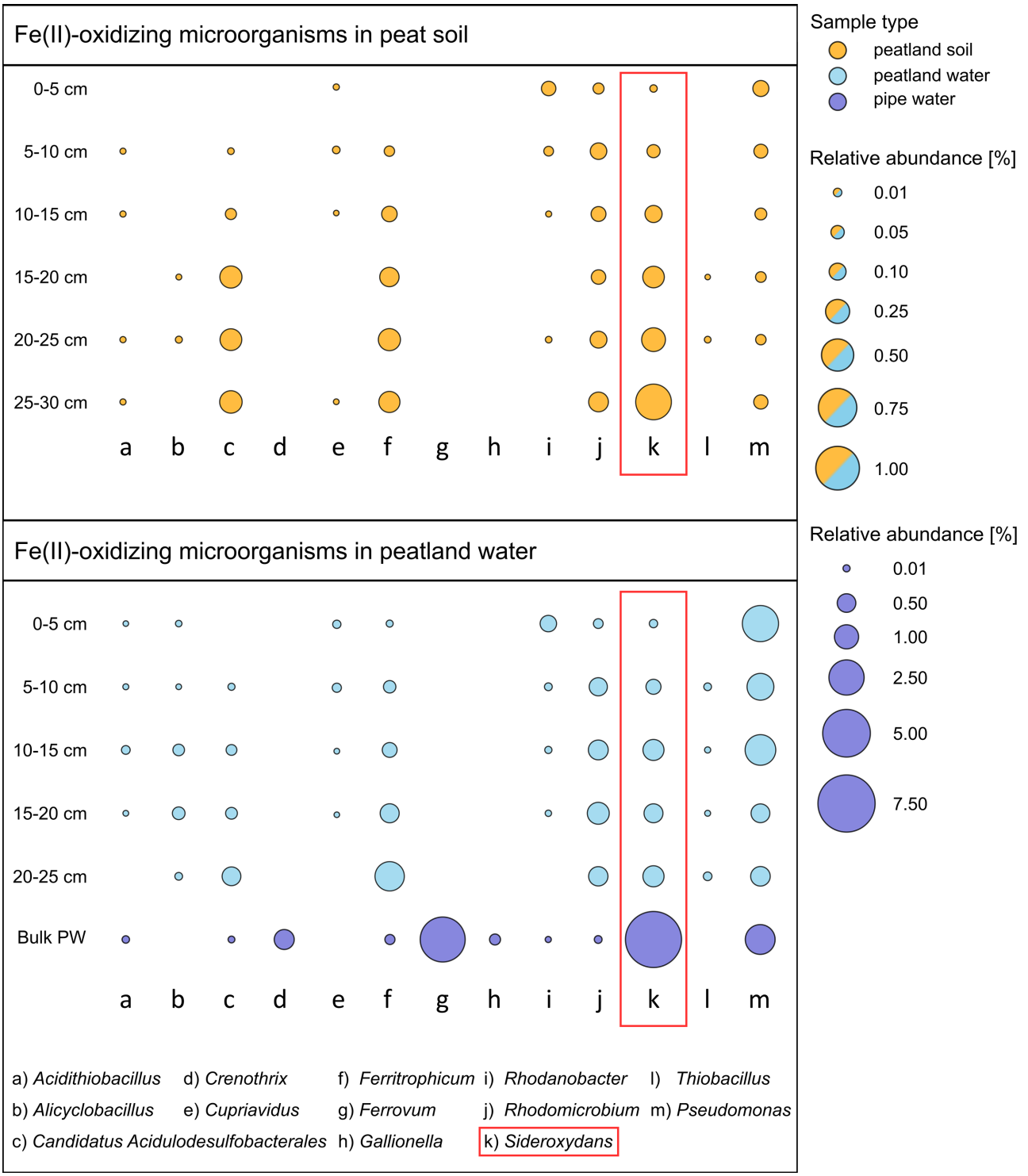

Figure 3. Relative abundances and depth distribution of Fe-metabolizing bacteria in peat soil fractions (0–30 cm), peat water fractions (0–30 cm), and standing water collected from a permanently installed pipe in the field. Dot plots representing the relative abundances of genus level groups of known FeOB found in the Schlöppnerbrunnen fen soil (top panel) and peatland water (bottom panel) fractions as shown for samples taken in 5 cm increments (0–5, 5–10, 10–15, 15–20, 20–25, 25–30 cm) and from standing water of a pipe. The replicates for each depth are grouped together for both soil and water fractions.

reducers has been reported in the Schlöppnerbrunnen fen (Loy *et al.* 2004), despite its low sulfate concentrations ranging from 25 to 100 μM (Knorr and Blodau 2009, Knorr *et al.* 2009). A rapid re-oxidation of reduced sulfur species has been postulated, fueling the activity of the sulfate-reducing keystone species *Desulfosporosinus* (Pester *et al.* 2010). Thus, *Sideroxydans* sp. CL21 is exposed to a great variety of inorganic and organic electron donors varying in time and space due to fluctuating redox conditions.

Sideroxydans sp. CL21 grows best with a combination of electron donors. Surprisingly, semi-solid incubations amended with lactate as the sole electron donor did not show significant growth; only in combination with inorganic electron donors like Fe, H_2, or thiosul-

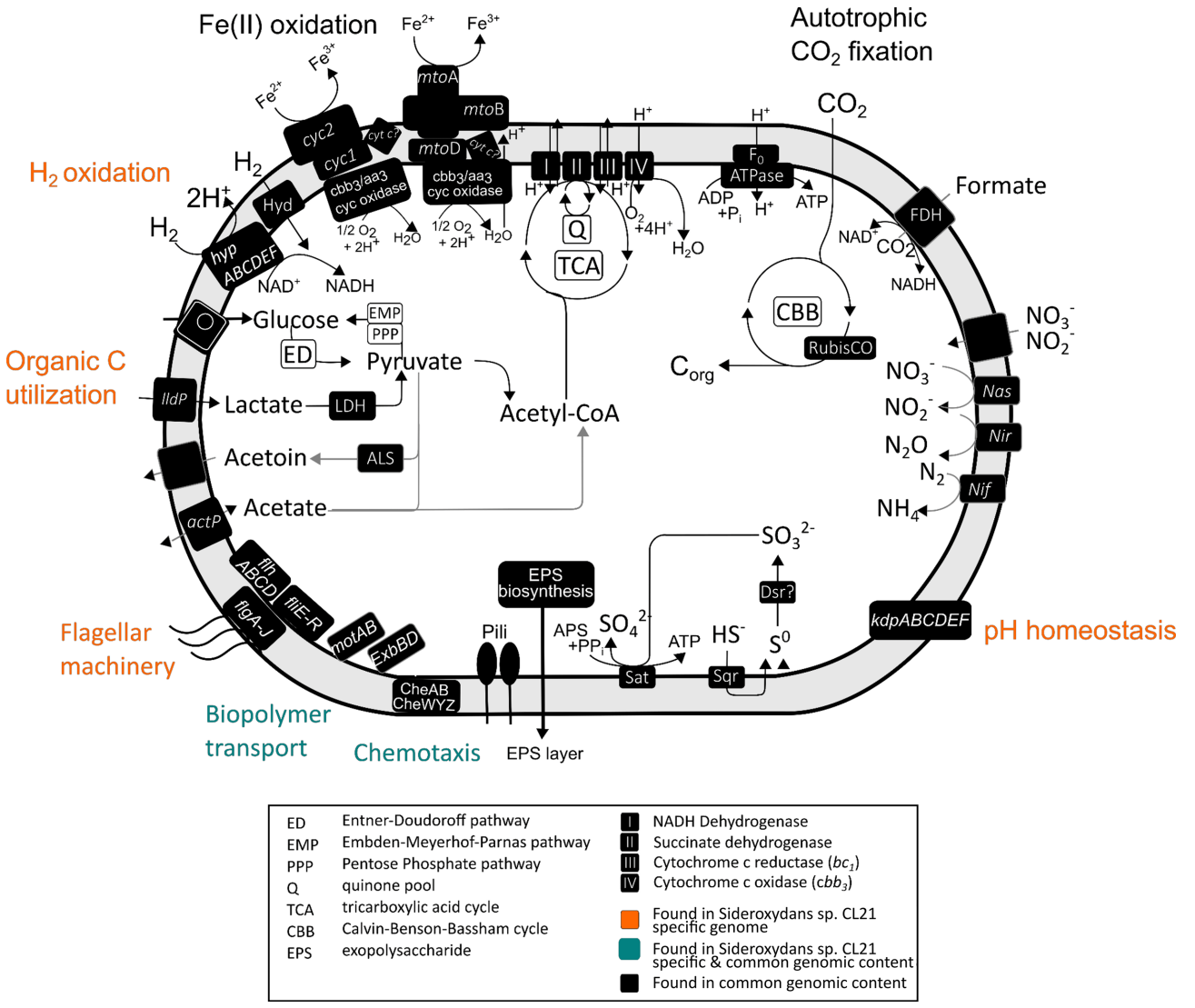

Figure 4. Graphical representation of potential metabolic activities in *Sideroxydans* sp. CL21 in comparison to the model FeOB *S. lithotrophicus* ES-1. The schematic is based solely on genome comparison analyses and represents metabolic pathways that are important for a mixotrophic metabolism in *Sideroxydans* sp. CL21 and suggests adaptation of this microbe to the slightly acidic, OM- and Fe-rich Schlöppnerbrunnen fen. Pathways highlighted in orange identified in the *Sideroxydans* sp. CL21 specific genome. Genes encoding biopolymer transport and chemotaxis were identified in both the common genomic content and specific genomes of *Sideroxydans* sp. CL21.

fate was growth observed. Thus, it remains unclear if *Sideroxydans* sp. CL21 is really able to channel lactate into a biosynthetic pathway using lactate dehydrogenase and to link lactate oxidation to energy conservation. Metagenomic contigs assigned to *Sideroxydans* strains of an acid mine drainage (AMD) enrichment culture also contained genes encoding for lactate utilization, lactate permease, but not for lactate dehydrogenase (Mühling *et al.* 2016). However, growth of *Sideroxydans* strains on organic acids, like lactate, in an AMD environment is not expected, as these organic acids are protonated under acidic conditions, and would release the proton upon entering the periplasm and likely damage the proton gradient across the cytoplasmic membrane (Muhling *et al.* 2016). As the pH of the Schlöppnerbrunnen fen varies between 4.5 and 5.5 (Reiche *et al.* 2008, Lüdecke *et al.* 2010, Hädrich *et al.* 2019), lactate would be already deprotonated due its low pKa of 3.9, and its uptake would not result in proton import.

Amendments with H_2 alone could stimulate growth of *Sideroxydans* sp. CL21, but H_2 consumption rates increased rapidly when Fe or particularly lactate were provided additionally. The highest H_2 consumption rate was observed with a combination of Fe and lactate. Simultaneous substrate utilization is not a unique feature for this strain. For example, the Fe(III) reducing microbe *Geobacter sulfurreducens* is capable of simultaneous utilization of H_2 and acetate under Fe(III)-reducing conditions (Brown *et al.* 2005). The capacity to prefer simultaneous utilization of a wide variety of inorganic and organic electron donors enables *Sideroxydans* sp. CL21 to make optimal use of the resources present in the fen, which are only available for a short period of time.

As *Sideroxydans* sp. CL21 is able to not only tolerate but prefer slightly acidic conditions of pH 5.5 (Lüdecke *et al.* 2010), strategies involved in maintaining pH homeostasis are important. We found the presence of multiple pathways in the *Sideroxydans* sp. CL21 accessory genome (i.e. *kdpABCDEF* operon and cyanophycin synthetases) to overcome acid stress (Fig. 4), similar to the findings in the above mentioned metagenomics study of *Sideroxydans* strains in a pH 3.5 enrichment culture (Muhling *et al.* 2016). The *kdpABCDEF* operon, a high-affinity potassium uptake system found in acidophiles, allows K+ to enter the cytoplasm, even when envi-

ronmental concentration is low, for maintenance of cytoplasmic K+ concentration which is necessary for pH homeostasis (Laimins *et al.* 1978, Epstein 1985, Muhling *et al.* 2016). The presence of cyanophycin synthetases in the *Sideroxydans* sp. CL21 accessory genome provides another mechanism for this microbe to respond to acidic conditions and maintain intracellular pH homeostasis, likely via enzymatic decarboxylation of protonated alpha-carboxy groups of cyanophycin arginine side chains, thereby creating a buffer against acidity and proton influx. The presence of different *Sideroxydans* strains in habitats spanning a wide pH range from pH neutral seeps (Emerson and Floyd 2005, Emerson *et al.* 2010), slightly acidic peatlands (Lüdecke *et al.* 2010, Kügler *et al.* 2019), to AMD affected environments (Lu *et al.* 2010, Fabisch *et al.* 2013, Mühling *et al.* 2016) demonstrates their strain specific adaptability to cope with acidic stress.

Another important genomic feature was the presence of genes linked to motility and chemotaxis in the accessory genome of *Sideroxydans* sp. CL21. Directed motion would enable strain CL21 to move along spatial geochemical gradients it deems attractive or away from surroundings it finds repellent in the semi-terrestrial environment. Our 16S rRNA amplicon sequence data revealed that *Sideroxydans* spp. are widespread throughout the peatland soil and peatland water across all depths with a preference for the deeper, water-saturated depths. Here they reach even 1% of the total relative abundance of the bacterial community. The presence of *Sideroxydans* spp. across all depths indicates the broad range of ecological niches *Sideroxydans* spp. occupies, since concentrations of O_2, Fe(II), thiosulfate, and fermentation products vary with depth and over time (Küsel *et al.* 2008, Reiche *et al.* 2010, Hausmann *et al.* 2016, Hausmann *et al.* 2018). The highest relative abundance of *Sideroxydans* spp. was detected in peatland water of an open pipe (up to 7% relative abundance), which might be related to the fact that the majority of known *Sideroxydans* spp. prefers to thrive in aquatic habitats.

We also found biofilm-related genes in the *Sideroxydans* sp. CL21 accessory genome. These genes were among the most up-regulated genes, when *Sideroxydans* sp. CL21 was incubated with the Fe(III) reducer *S. oneidensis* (Cooper *et al.* 2020b). Surprisingly, genes related to the iron oxidation and reduction machinery were not differentially expressed during this co-cultivation experiment. Shaping the environment by a regulated inter-species biofilm formation appears to be the key mechanism underlying interactions of these Fe-cycling microorganisms (Cooper *et al.* 2020b).

Niche partitioning by various ecotypes within the genus *Sideroxydans* as well as metabolic pathway diversity within a strain (e.g. different metabolic pathways for energy production) seems to be a useful means of survival. Overall, our combined data suggest an evolutionary process leading to gene acquisition driven by the adaptation to a slightly acidic, OM-rich semi-terrestrial ecosystem, characterized by typically changing water table levels, steep O_2 gradients, and an anaerobic turnover of organic carbon. We found several transposase elements in the accessory genome of *Sideroxydans* sp. CL21. For example, a transposase and an integrase located upstream and downstream of the high affinity potassium uptake system encoding the *kdpABCDEF* gene cluster, which is involved in maintaining pH homeostasis in acidic environments, indicates that this gene cluster may have been acquired via horizontal gene transfer. Larger genome size allows adaptation of microorganisms to nutrient rich and fluctuating environmental conditions (Bentkowski *et al.* 2015, Cobo-Simon and Tamames 2017). Genera detected in soils typically have larger genome sizes, in comparison to genera from oligotrophic freshwater or marine environments (Cobo-Simon and Tamames 2017). These differences have been mainly attributed to differences in habitat complexity and/or nutrient availability (Konstantinidis and Tiedje 2004, DeLong *et al.* 2006, Okie *et al.* 2020). Collectively, the data from our genome comparison study and incubation experiments suggest that *Sideroxydans* sp. CL21 is perfectly adapted to its semi-terrestrial habitat.

Implications

This novel genomic insight enabled targeted experiments to corroborate physiological and metabolic potentials. The diverse metabolic and physiological potential of *Sideroxydans* sp. CL21 highlights the importance of metabolic flexibility for microorganisms which inhabit environments characterized by fluctuating redox conditions as well as high concentrations of OM and copious amounts of diverse electron donors, electron acceptors, and electron shuttles.

Supplementary data

Supplementary data are available at *FEMSEC* online.

Acknowledgments

We thank Alison Favaroni for editorial assistance and Jens D Wurlitzer for his invaluable technical assistance in the laboratory and during sample collection in the Schlöppnerbrunnen fen.

Conflict of interest. None declared.

Funding

REC, JF, and KK were supported by the Collaborative Research Centre Chemical Mediators in Complex Biosystems (SFB 1127 ChemBioSys, Project Number 239748522), which is funded by the Deutsche Forschungsgemeinschaft. CSC was supported by the National Science Foundation (EAR-1833525).

References

Alewell C, Paul S, Lischeid G *et al.* Characterizing the redox status in three different forested wetlands with geochemical data. *Environ Sci Technol* 2006;**40**:7609–15.

Apprill A, McNally S, Parsons R *et al.* Minor revisin to V4 region SSU rRNA 806R gene primer greatly increases detection of SAR11 bacterioplankton. *Aquat Microb Ecol* 2015;**75**:129–37.

Aziz RK, Bartels D, Best AA *et al.* The RAST Server: rapid annotations using subsystems technology. *BMC Genomics* 2008;**9**:75.

Badger MR, Bek EJ. Multiple Rubisco forms in proteobacteria: their functional significance in relation to CO2 acquisition by the CBB cycle. *J Exp Bot* 2008;**59**:1525–41.

Beckwith CR, Edwards MJ, Lawes M *et al.* Characterization of MtoD from *Sideroxydans lithotrophicus*: a cytochrome c electron shuttle used in lithoautotrophic growth. *Frontiers in Microbiology* 2015;**6**:332.

Bentkowski P, Van Oosterhout C, Mock T. A model of genome size evolution for prokaryotes in stable and fluctuating environments. *Genome Biol Evolut* 2015;**7**:2344–51.

Bethencourt L, Bochet O, Farasin J *et al.* Genome reconstruction reveals distinct assemblages of Gallionellaceae in surface and subsurface redox transition zones. *FEMS Microbiol Ecol* 2020;**96**. doi: 10.1093/femsec/fiaa036..

Blodau C, Roehm C.L., Moore T.R. Iron, sulfur, and dissolved carbon dynamics in a northern peatland. *Fundam Appl Limnol* 2002;**154**:561–83.

Bodelier PLE, Frenzel P, Drake HL *et al.* Ecological aspects of microbes and microbial communities inhabiting the rhizosphere of wetland plants. *Wetlands and Natural Resource Management* 2006;205–38.

Bragazza L, Parisod J, Buttler A *et al.* Biogeochemical plant-soil microbe feedback in response to climate warming in peatlands. *Nature Climate Change* 2013;**3**:273–7.

Brettin T, Davis JJ, Disz T *et al.* RASTtk: a modular and extensible implementation of the RAST algorithm for building custom annotation pipelines and annotating batches of genomes. *Sci Rep* 2015;**5**:8365.

Brown DG, Komlos J, Jaffe PR. Simultaneous utilization of acetate and hydrogen by *Geobacter sulfurreducens* and implications for use of hydrogen as an indicator of redox conditions. *Environ Sci Technol* 2005;**39**:3069–76.

Bryce C, Blackwell N, Schmidt C *et al.* Microbial anaerobic Fe(II) oxidation - Ecology, mechanisms and environmental implications. *Environ Microbiol* 2018;**20**:3462–83.

Caporaso JG, Lauber CL, Walters WA *et al.* Global patterns of 16S rRNA diversity at a depth of millions of sequences per sample. *Proc Natl Acad Sci* 2011;**108**:4516–22.

Caporaso JG, Lauber CL, Walters WA *et al.* Ultra-high-throughput microbial community analysis on the Illumina HiSeq and MiSeq platforms. *ISME J* 2012;**6**:1621–4.

Carere CR, Hards K, Houghton KM *et al.* Mixotrophy drives niche expansion of verrucomicrobial methanotrophs. *ISME J* 2017;**11**:2599–610.

Chan CS, McAllister SM, Leavitt AH *et al.* The architecture of iron microbial mats reflects the adaptation of chemolithotrophic iron oxidation in freshwater and marine environments. *Frontiers in Microbiology* 2016;**7**:796.

Cheng Q, Huang Y, Nengzi L *et al.* Performance and microbial community pro-files in pilot-scale biofilter for ammonia, iron and manganese removal at different dissolved oxygen concentrations. *World J Microbiol Biotechnol* 2019;**35**:1–11.

Cobo-Simon M, Tamames J. Relating genomic characteristics to environmental preferences and ubiquity in different microbial taxa. *BMC Genomics* 2017;**18**:499.

Cooper RE, Wegner CE, McAllister SM *et al.* Draft genome sequence of *Sideroxydans* sp. strain CL21, an Fe(II)-oxidizing bacterium. *Microbiol Resour Announc* 2020a;**9**:e01444–19.

Cooper RE, Wegner CE, Kügler S *et al.* Iron is not everything: unexpected complex metabolic responses between iron-cycling microorganisms. *ISME J* 2020b;**14**:2675–90.

Coppi MV, O'Neil RA, Lovley DR. Identification of an uptake hydrogenase required for hydrogen-dependent reduction of Fe(III) and other electron acceptors by *Geobacter sulfurreducens*. *J Bacteriol* 2004;**186**:3022–8.

Delmont TO, Eren AM. Linking pangenomes and metagenomes: the prochlorococcus metapangenome. *Peer J* 2018;**6**:e4320.

DeLong EF, Preston CM, Mincer T *et al.* Community genomics among stratified microbial assemblages in the ocean's interior. *Science* 2006;**311**:496–503.

Dibrova DV, Galperin MY, Mulkidjanian AY Characterization of the N-ATPase, a distinct, laterally transferred Na^+-translocating form of the bacterial F-type membrane atpase. *Bioinformatics* 2010;**26**:1473–6.

Drake HL, Horn MA, Wüst PK Intermediary ecosystem metabolism as a main driver of methanogenesis in acidic wetland soil. *Environ Microbiol Rep* 2009;**1**:307–18.

Druschel GK, Emerson D, Sutka R *et al.* Low-oxygen and chemical kinetic constraints on the geochemical niche of neutrophilic iron(II) oxidizing microorganisms. *Geochim Cosmochim Acta* 2008;**72**:3358–70.

Edgar R. Search and clustering orders of magnitude faster than BLAST. *Bioinformatics* 2010;**26**:2460–1.

Eggerichs T, Wiegand M, Neumann K *et al.* Growth of iron-Oxidizing bacteria *Gallionella ferruginea* and *Leptothrix cholodnii* in oligotrophic environments: Ca, Mg, and C as limiting factors and *G. ferruginea* necromass as C-Source. *Geomicrobiol J* 2020;**37**:190–9.

Emerson D, Moyer C. Isolation and characterization of novel iron-oxidizing bacteria that grow at circumneutral pH. *Appl Environ Microbiol* 1997;**63**:4784–92.

Emerson D, Floyd MM. Enrichment and isolation of iron-oxidizing bacteria at neutral pH. *Methods Enzymol* 2005;**397**:112–23.

Emerson D, Fleming EJ, McBeth JM. Iron-oxidizing bacteria: an environmental and genomic perspective. *Annu Rev Microbiol* 2010;**64**:561–83.

Emerson D, Field EK, Chertkov O *et al.* Comparative genomics of freshwater Fe-oxidizing bacteria: implications for physiology, ecology, and systematics. *Frontiers in Microbiology* 2013;**4**:254.

Epstein W. Chapter 9 the Kdp system: a bacterial K+ transport atpase. *Current Topics in Membranes and Transport*, Academic Press: Elsevier, 1985;**23**:153–75.

Eren AM, Esen OC, Quince C *et al.* Anvi'o: an advanced analysis and visualization platform for 'omics data. *PeerJ* 2015;**3**:e1319.

Eren AM, Kiefl E, Shaiber A *et al.* Community-led, integrated, reproducible multi-omics with anvi'o. *Nature Microbiology* 2021;**6**:3–6.

Fabisch M, Beulig F, Akob DM *et al.* Surprising abundance of *Gallionella*-related iron oxidizers in creek sediments at pH 4.4 or at high heavy metal concentrations. *Frontiers in Microbiology* 2013;**4**:390.

Fleming EJ, Cetinić I, Chan CS *et al.* Ecological succession among iron-oxidizing bacteria. *ISME J* 2014;**8**:804–15.

Garber AI, Nealson KH, Okamoto A *et al.* FeGenie: a comprehensive tool for the identification of iron genes and iron gene neighborhoods in genome and metagenome assemblies. *Frontiers in Microbiology* 2020;**11**:37.

Graham ED, Heidelberg JF, Tully BJ. Potential for primary productivity in a globally-distributed bacterial phototroph. *ISME J* 2018;**12**:1861–6.

Hädrich A, Heuer VB, Herrmann M *et al.* Origin and fate of acetate in an acidic fen. *FEMS Microbiol Ecol* 2012;**81**:339–54.

Hädrich A, Taillefert M, Akob DM *et al.* Microbial Fe(II) oxidation by *Sideroxydans lithotrophicus* ES-1 in the presence of Schlöppnerbrunnen fen-derived humic acids. *FEMS Microbiol Ecol* 2019;**95**. doi: 10.1093/femsec/fiz034.

Hamberger A, Horn MA, Dumont MG *et al.* Anaerobic consumers of monosaccharides in a moderately acidic fen. *Appl Environ Microbiol* 2008;**74**:3112–20.

Hartmann S, Frielingsdorf S, Ciaccafava A *et al.* O_2-Tolerant H_2 activation by an isolated large subunit of a [NiFe] hydrogenase. *Biochemistry* 2018;**57**:5339–49.

Hausinger RP. Metabolic versatility of prokaryotes for urea decomposition. *J Bacteriol* 2004;**186**:2520–2.

Hausmann B, Knorr KH, Schreck K *et al.* Consortia of low-abundance bacteria drive sulfate reduction-dependent degradation of fermentation products in peat soil microcosms. *ISME J* 2016;**10**:2365–75.

Hausmann B, Pelikan C, Herbold CW *et al.* Peatland acidobacteria with a dissimilatory sulfur metabolism. *ISME J* 2018;**12**:1729–42.

He S, Barco RA, Emerson D *et al.* Comparative genomic analysis of neutrophilic iron(II) oxidizer genomes for candidate genes in extracellular electron transfer. *Frontiers in Microbiology* 2017;**8**:1584.

Huang YM, Jakus N, Straub D *et al.*'Candidatus ferrigenium straubiae' sp. nov., 'Candidatus ferrigenium bremense' sp. nov., 'Candidatus ferrigenium altingense' sp. nov., are autotrophic Fe(II)-oxidizing bacteria of the family Gallionellaceae. *Syst Appl Microbiol* 2022;**45**:126306.

Ilbert M, Bonnefoy V. Insight into the evolution of the iron oxidation pathways. *Biochimica Et Biophysica Acta (BBA) - Bioenergetics* 2013;**1827**:161–75.

Johnson DB, Kanao T, Hedrich S. Redox transformations of iron at extremely low pH: fundamental and applied aspects. *Front Microbiol* 2012;**3**:96.

Kanamori T, Kanou N, Kusakabe S *et al.* Allophanate hydrolase of *Oleomonas sagaranensis* involved in an ATP-dependent degradation pathway specific to urea. *FEMS Microbiol Lett* 2005;**245**:61–5.

Keffer JL, McAllister SM, Garber AI *et al.* Iron oxidation by a fused cytochrome-porin common to diverse iron-oxidizing bacteria. *Mbio* 2021;**12**:e0107421.

Klindworth A, Pruesse E, Schweer T *et al.* Evaluation of general 16S ribosomal RNA gene PCR primers for classical and next-generation sequencing-based diversity studies. *Nucleic Acids Res* 2013;**41**:e1.

Knorr KH, Blodau C. Impact of experimental drought and rewetting on redox transformations and methanogenesis in mesocosms of a northern fen soil. *Soil Biol Biochem* 2009;**41**:1187–98.

Knorr KH, Lischeid G, Blodau C. Dynamics of redox processes in a minerotrophic fen exposed to a water table manipulation. *Geoderma* 2009;**153**:379–92.

Konstantinidis KT, Tiedje JM. Trends between gene content and genome size in prokaryotic species with larger genomes. *Proc Natl Acad Sci* 2004;**101**:3160–5.

Krehenbrink M, Oppermann-Sanio FB, Steinbuchel A. Evaluation of non-cyanobacterial genome sequences for occurrence of genes encoding proteins homologous to cyanophycin synthetase and cloning of an active cyanophycin synthetase from *Acinetobacter* sp. strain DSM 587. *Arch Microbiol* 2002;**177**:371–80.

Kügler S, Cooper RE, Wegner CE *et al.* Iron-organic matter complexes accelerate microbial iron cycling in an iron-rich fen. *Sci Total Environ* 2019;**646**:972–88.

Kügler S, Cooper RE, Boessneck J *et al.* Rhizobactin B is the preferred siderophore by a novel *Pseudomonas* isolate to obtain iron from dissolved organic matter in peatlands. *Biometals* 2020;**33**:415–33.

Küsel K, Blöthe M, Schulz D *et al.* Microbial reduction of iron and porewater biogeochemistry in acidic peatlands. *Biogeosciences* 2008;**5**:1537–49.

Laimins LA, Rhoads DB, Altendorf K *et al.* Identification of the structural proteins of an ATP-driven potassium transport system in *Escherichia coli*. *Proc Natl Acad Sci* 1978;**75**:3216–9.

Lee YP, Fujii M, Kikuchi T *et al.* Importance of allochthonous and autochthonous dissolved organic matter in Fe(II) oxidation: a case study in Shizugawa Bay watershed, Japan. *Chemosphere* 2017;**180**:221–8.

Li Y, Raschdorf O, Silva KT *et al.* The terminal oxidase cbb3 functions in redox control of magnetite biomineralization in *Magnetospirillum gryphiswaldense*. *J Bacteriol* 2014;**196**:2552–62.

Liu J, Wang Z, Belchik SM *et al.* Identification and characterization of MtoA: a decaheme c-type cytochrome of the neutrophilic Fe(II)-oxidizing bacterium *Sideroxydans lithotrophicus* ES-1. *Frontiers in Microbiology* 2012;**3**:37.

Loy A, Küsel K, Lehner A *et al.* Microarray and functional gene analyses of sulfate-reducing prokaryotes in low-sulfate, acidic fens reveal cooccurrence of recognized genera and novel lineages. *Appl Environ Microbiol* 2004;**70**:6998–7009.

Lu S, Gischkat S, Reiche M *et al.* Ecophysiology of Fe-cycling bacteria in acidic sediments. *Appl Environ Microbiol* 2010;**76**:8174–83.

Lüdecke C, Reiche M, Eusterhues K *et al.* Acid-tolerant microaerophilic Fe(II)-oxidizing bacteria promote Fe(III)-accumulation in a fen. *Environ Microbiol* 2010;**12**:2814–25.

McAllister SM, Polson SW, Butterfield DA *et al.* Validating the Cyc2 neutrophilic iron oxidation pathway using meta-omics of zetaproteobacteria iron mats at marine hydrothermal vents. *Msystems* 2020;**5**. https://doi.org/10.1128/mSystems.00553-19.

Meier AB, Oppermann S, Drake HL *et al.* Organic carbon from graminoid roots as a driver of fermentation in a fen. *FEMS Microbiol Ecol* 2021;**97**. doi: 10.1093/femsec/fiab143.

Mitra A, Flynn KJ, Burkholder JM *et al.* The role of mixotrophic protists in the biological carbon pump. *Biogeosciences* 2014;**11**:995–1005.

Mühling M, Poehlein A, Stuhr A *et al.* Reconstruction of the metabolic potential of acidophilic sideroxydans strains from the metagenome of an microaerophilic enrichment culture of acidophilic iron-oxidizing bacteria from a pilot plant for the treatment of acid mine drainage reveals metabolic versatility and adaptation to life at low pH. *Front Microbiol* 2016;**7**:2082.

Okie JG, Poret-Peterson AT, Lee ZM *et al.* Genomic adaptations in information processing underpin trophic strategy in a whole-ecosystem nutrient enrichment experiment. *Elife* 2020;**9**. https://doi.org/10.7554/eLife.49816.

Otte J, Harter J, Laufer K *et al.* The distribution of active iron-cycling bacteria in marine and freshwater sediments is decoupled from geochemical gradients. *Environ Microbiol* 2018;**20**:2483–99.

Overbeek R, Olson R, Pusch GD *et al.* The SEED and the rapid annotation of microbial genomes using Subsystems Technology (RAST). *Nucleic Acids Res* 2014;**42**:D206–214.

Parada AE, Needham DM, Fuhrman JA. Every base matters: assessing small subunit rRNA primers for marine microbiomes with mock communities, time series and global field samples. *Environ Microbiol* 2016;**18**:1403–14.

Park SJ, Andrei AS, Bulzu PA *et al.* Expanded diversity and metabolic versatility of marine nitrite-oxidizing bacteria revealed by cultivation- and genomics-based approaches. *Appl Environ Microbiol* 2020;**86**. https://doi.org/10.1128/AEM.01667-20.

Paul S, Küsel K, Alewell C. Reduction processes in forest wetlands: tracking down heterogeneity of source/sink functions with a combination of methods. *Soil Biol Biochem* 2006;**38**:1028–39.

Pester M, Bittner N, Deevong P *et al.* A 'rare biosphere' microorganism contributes to sulfate reduction in a peatland. *ISME J* 2010;**4**:1591–602.

Peters JW, Schut GJ, Boyd ES *et al.*[FeFe]- and [NiFe]-hydrogenase diversity, mechanism, and maturation. *Biochimica Et Biophysica Acta (BBA) - Mol Cell Res* 2015;**1853**:1350–69.

Pitcher RS, Brittain T, Watmough NJ. Cytochrome cbb(3) oxidase and bacterial microaerobic metabolism. *Biochem Soc Trans* 2002;**30**:653–8.

Reiche M, Torburg G, Küsel K. Competition of Fe(III) reduction and methanogenesis in an acidic fen. *FEMS Microbiol Ecol* 2008;**65**:88–101.

Reiche M, Gleixner G, Küsel K. Effect of peat quality on microbial greenhouse gas formation in an acidic fen. *Biogeosciences* 2010;**7**:187–98.

Riedel T, Zak D, Biester H *et al.* Iron traps terrestrially derived dissolved organic matter at redox interfaces. *Proc Natl Acad Sci* 2013;**110**:10101–5.

Rodriguez-R LM, Konstantinidis KT. The enveomics collection: a toolbox for specialized analyses of microbial genomes and metagenomes. *PeerJ Preprints* 2016;**4**:e1900v1. https://doi.org/10.7287/peerj.preprints.1900v1.

Rognes T, Flouri T, Nichols B *et al.* VSEARCH: a versatile open source tool for metagenomics. *PeerJ* 2016;**4**:e2584.

Roller BR, Schmidt TM. The physiology and ecological implications of efficient growth. *ISME J* 2015;**9**:1481–7.

RStudio Team. RStudio: Integrated Development for R. RStudio, PBC, Boston, MA URL. 2020; URL: http://www.rstudio.com/.

Shafaat HS, Rudiger O, Ogata H *et al.*[NiFe] hydrogenases: a common active site for hydrogen metabolism under diverse conditions. *Biochimica Et Biophysica Acta (BBA) - Bioenergetics* 2013;**1827**:986–1002.

Taubert M, Stöckel S, Geesink P *et al.* Tracking active groundwater microbes with D_2O labelling to understand their ecosystem function. *Environ Microbiol* 2018;**20**:369–84.

Till BA, Weathers LJ, Alvarez PJJ. Fe(0)-supported autotrophic denitrification. *Environ Sci Technol* 1998;**32**:634–9.

Ullrich SR, Poehlein A, Tischler JS *et al.* Genome analysis of the biotechnologically relevant acidophilic iron oxidising strain JA12 indicates phylogenetic and metabolic diversity within the novel genus "*Ferrovum*". *PLoS One* 2016;**11**:e0146832.

Weber KA, Achenbach LA, Coates JD. Microorganisms pumping iron: anaerobic microbial iron oxidation and reduction. *Nat Rev Microbiol* 2006;**4**:752–64.

Wickham H. *Ggplot2: elegant graphics for Data analysis*. *Springer Cham*, 2016.

Wüst PK, Horn MA, Drake HL. Trophic links between fermenters and methanogens in a moderately acidic fen soil. *Environ Microbiol* 2009;**11**:1395–409.

Xu L, Dong Z, Fang L *et al.* OrthoVenn2: a web server for whole-genome comparison and annotation of orthologous clusters across multiple species. *Nucleic Acids Res* 2019;**47**:W52–8.

Yang L, Jiang M, Zou Y *et al.* Geographical distribution of iron redox cycling bacterial community in peatlands: distinct assemble mechanism across environmental gradient. *Front Microbiol* 2021;**12**:674411.

Zhou N, Keffer JL, Polson SW *et al.* Unraveling Fe(II)-oxidizing mechanisms in a facultative Fe(II) oxidizer, *Sideroxydans lithotrophicus* strain ES-1, via culturing, transcriptomics, and reverse transcription-quantitative PCR. *Appl Environ Microbiol* 2022;**88**:e0159521.